ELSEVIER

Journal of Chromatography A, 923 (2001) 119–126

JOURNAL OF CHROMATOGRAPHY A

www.elsevier.com/locate/chroma

Size- and shape-dependent separation of TiO_2 colloidal sub-populations with gravitational field flow fractionation

Sousan Rasouli[a], Philippe Blanchart[b], Dominique Clédat[a], Philippe J.P. Cardot[a,*]

[a]*Laboratoire de Chimie Analytique et de Bromatologie, Université de Limoges Faculté de Pharmacie, 2 Rue du Dr Marcland, F-87025 Limoges Cedex, France*

[b]*GEMH, Ecole Nationale Supérieure de Céramique Industrielle, 47–73 Avenue Albert Thomas, 87065 Limoges Cedex, France*

Received 8 February 2001; received in revised form 17 May 2001; accepted 17 May 2001

Abstract

The simplest field flow fractionation technique, which uses the earth's gravity as the external field is applied to isolate two populations, which differ in both shape and size, from a polydisperse sub-micron TiO_2 powder of homogenous density. The fraction eluted first is spherical with an average diameter of 0.31 μm while the second fraction is ellipsoidal and can be associated with a 0.45 μm hydrodynamic diameter. Elution conditions appeared to be very sensitive to electrolyte and surfactant characteristics in the carrier phase as well as on the sample concentration. Using 25 μl (1%, w/w) sample suspension, separations of spherical from ovoid particles was performed in almost 2 h with a mobile phase of 0.001 *M* KNO_3–0.01% (v/v) Fl-70 in water in a 0.025-cm thick channel made of polystyrene walls.

Keywords: Gravitational field-flow fractionation; Field-flow fractionation; Titanium oxide

1. Introduction

Sedimentation field flow fractionation (FFF) is an analytical technique able to separate a large variety of colloids [1–3]. Sedimentation FFF with multi-gravitational field (SdFFF) was recently used to characterise 20 nm diameter gold particles [4] as well as to obtain purified fractions of reduced dispersities from a sub-micron TiO_2 sample [5]. Gravitational field flow fractionation (GFFF) is a subset of sedimentation FFF techniques. Its main advantages lie in its design and operating simplicity. It uses simple earth gravity as external field and is raising interest, because of the relative confidentiality in the use of FFF, for micron and sub-micron sized particle separation. GFFF can be considered, at least, as the basic and primary technique if one wants to enter the FFF world at low cost. Otherwise it shows constant spreading of applications [6–8].

If most of the GFFF applications refer to the selective elution and separation of micron sized species, sub-micron particles can be expected to be fractionated using GFFF for all those species having a mass that allows interaction with the external field. TiO_2 colloidal suspensions in the 100–600 nm diameter range, with density 4.2 g/cm^3, belong to this category. The elution mode of this population is expected to be Brownian [9] as already demonstrated

*Corresponding author. Tel.: +33-5-5543-5857; fax: +33-5-5543-5859.

E-mail address: cardot@unilim.fr (P.J.P. Cardot).

0021-9673/01/$ – see front matter
PII: S0021-9673(01)00970-0

with other sedimentation FFF techniques operated at high or moderated multi-gravitational fields [5,10].

Titanium oxide powder is widely used as a pigment or ceramic material because of its inert chemical properties, high refractive index and hiding power. When it is used as a white pigment, properties depend on the scattering of light from small particles embedded in a transparent medium and then, the diffuse reflectance is a function of the grain size distribution [11]. For ceramics, the sintering of the fine grained microstructure is particularly controlled by the grain size distribution and their aspect ratio. Sintered ceramics with well define pore structure can be used for sub-micron filtering [12].

In general, many powder formulations are under the form of disperse systems such as colloidal suspensions for which the stability is governed by the material itself and the liquid, but also by the grain size distribution [13]. A theoretical description of particle dispersion in a liquid can be approached through models including parameters as the grain size. For example, it was shown that the dielectric properties at high frequency of concentrated TiO_2 suspensions [14] could be characterised using well known sub-micron particles.

The objectives of this report rely on the investigation of the separation power of GFFF on a very polydisperse colloidal sample (TiO_2) using independent sizing methods. It is known that for colloidal suspensions, carrier phase electrolyte and surfactant composition played critical roles, modulating particles retention properties as well as sample recovery [15–17]. The complex particle–particle and particle–wall interaction effects already described [16,17], depend, indeed, on the above conditions. However they will be discussed only in terms of separation enhancement.

2. Experimental

2.1. TiO_2 colloidal sample

The sample used in this report was already described by Cardot et al. in a recent paper [5]. Particle size distribution showed a continuous and monomodal diameter distribution between 0.1 and 0.6 μm with an average value of 0.32 μm. The average density of the whole sample, as well as of the SdFFF fractions was measured to be 4.3 g/cm^3. The refractive index of the colloidal sample was measured to be RI=2.

2.2. GFFF separation system

The GFFF separator design and relevant set up was already described in other papers [18–20]. It must be recalled here that the channel walls are made of two polystyrene plates separated by a Mylar spacer 0.025 cm thick in which a 50×1 cm channel with tapered ends is manually cut. The other particularity of this GFFF channel, is that inlet and outlet tubings are both glued on the accumulation wall. Thus, sample inlet is at the accumulation wall. This separator simply replaces the high-performance liquid chromatography (HPLC) column of a classical liquid chromatographic system. This is equipped with an HPLC pump Gilson Model 302 (Gilson Medical Electronics, Middeltown, WI, USA), a 25-μl loop Rheodyne valve Model 7125i (Rheodyne, Cotati, CA, USA) and a differential refractometer ICS Model M81110 (ICS, Lauganet, France). Signals were recorded by means of a computer assisted data acquisition system already described [21].

The carrier phase is made of doubly distilled water mixed with different percentages of FL70 surfactant (Fisher Scientific, Springfield, NJ, USA) and KNO_3 (ACS reagent, Sigma–Aldrich, St. Quentin Fallavier, France). When needed, fractions were manually collected at different elution time and size analysis made after scanning electron microscopy (SEM) of the fractions. The electron microscopy (EM) system was a Hitachi S-2500 (Hitachi, Tokyo, Japan). EM sizing algorithms were already described [5].

2.3. FFF methodology

Elution of species in the ''Brownian'' elution mode [9] requires a specific injection procedure described as ''Stop flow injection''. In this procedure, when the sample is introduced into the channel (and this requires the precise knowledge of the volume of injection valve to channel connection tubing and of the pump flow-rate), the flow is stopped to allow the sample to sediment across the channel thickness. This, can be practically made by

inserting, between the pump and the injection device, a three-way valve Model V100L (Upchurch Scientific, Oak Harbor, WA, USA). After the introduction, the sample settles under the influence of the external field until an equilibrium state is reached. The time required to obtain that equilibrium is called the primary relaxation time (also often reported as stop flow time). If some properties of the sample to be eluted in GFFF are known, i.e., size distribution and average density, this stop flow time can be calculated. Being a sedimentation process, it is just the time required for the sample particle of lowest mass to travel, under the effect of the just earth's gravity field from the depletion wall to the accumulation wall [22]. Some authors recommend employing a stop flow time of twice the relaxation time [23]. However, this over evaluation is related to the classical design of channels, in which the inlet tubing which is glued at the upper wall. The stop flow time for TiO_2 in such a classical configuration will be 234 min for the smallest particles [23]. It is, indeed, possible to drastically reduce the stop flow time by introducing the sample at a very low flow-rate directly from the accumulation wall. This can be done by gluing the inlet tubing on the accumulation wall.

3. Results and discussion

3.1. Separation of spherical and ovoid sub-micron TiO_2 particles

GFFF of the TiO_2 polydisperse sample led to the characteristic fractogram shown in Fig. 1. As TiO_2 is eluted, in SdFFF at high external fields, with the ''Brownian'' elution mode [5,9], it is assumed here that also in GFFF, the elution mode is of the same type. With a known density of 4.2 g/cm^3, it is possible to derive the average hydrodynamic size of the eluted TiO_2 from the retention time or the elution volume according to the basic equations defined by Schure et al. [9]. The calculated size values along the fractogram are reported in Fig. 1. Two major peaks can be evidenced (a and b). From their retention ratios it is possible to calculate their expected hydrodynamic diameter values, which were found to be, respectively, at 0.314 μm and 0.455 μm. The

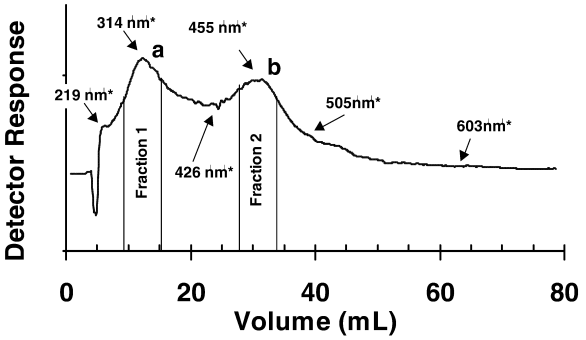

Fig. 1. Elution profile of TiO_2 colloid in GFFF. Sample: 25 ml (1%, w/w) TiO_2 colloidal suspension in carrier phase. GFFF separator: 50×1×0.025 cm, system void volume of 1.55 ml measured with 10% (w/w) Dextran (T500) solution. Carrier phase: KNO_3 (0.001 *M*)–FL-70 (0.01%, v/w)–bidistilled water. Flow-rate: 1 ml/min. Detector attenuation 100 (detector range: 1–2000), stop flow time: 40 min.

accuracy of this sizing methodology is controlled by collecting 6.5 ml for each fraction eluted in correspondence of peak summits a (fraction 1) and b (fraction 2), as shown in Fig. 1. Microscopy pictures of the collected fractions are shown in Fig. 2.

Electron microscopy size measurements (SEM) performed on collected particles gave the value of 0.319 μm for the spherical particles of fraction 1. The polydispersity index is <5%. For fraction 2, the

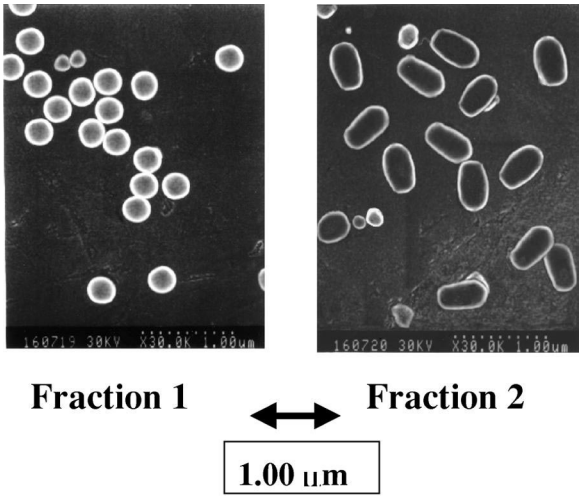

Fig. 2. TiO_2 scanning electron microscopy of sample fractions 1 and 2. Hitachi S-2500 scanning electron microscope, magnification ×30 000. The photos represent 25% of the scanned field.

ovoid particles present two major dimensions, measured as the length and the breadth, whose respective values are 565 nm and 347 nm (with a polydispersity index <5%). In that case, the average value is equivalent to a hydrodynamic diameter of 456 nm. Size values for both fractions are, thus, very close to the calculated values obtained by means of the retention expression for the Brownian elution model as shown in Fig. 2.

3.2. Separation enhancement: critical parameters

Four different critical parameters were studied for the separation enhancement between 0.45 μm ovoid particles and 0.32 μm spherical ones. The first one consists in the determination of the best stop flow time value, the second is related to the determination of the highest particle sample amount to be introduced into the channel with enhanced effect on separation selectivity. The third and fourth are related to the search of the best carrier phase composition.

3.2.1. Determination of the best stop flow time value

The sample is introduced into the channel at low flow-rate (0.2 ml/min), for a time corresponding to the injection loop and inlet connection tubing volume. Flow is stopped by means of the three-way valve described above. After sample relaxation, the flow is then resumed into the channel at the chosen elution flow (1 ml/min) by means of the three-way valve. Elution profiles obtained for four different stop flow times are given in Fig. 3.

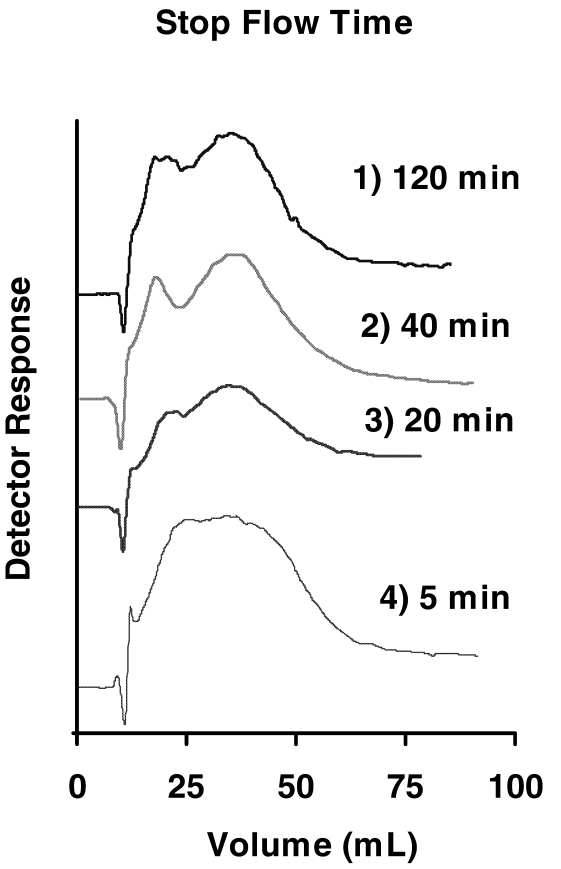

Fig. 3. Stop flow time dependent elution profile of TiO_2 colloid in GFFF. Sample: 25 μl (1%, w/w) TiO_2 colloidal suspension in the carrier phase. GFFF separator: 50×1×0.025 cm, system void volume of 1.55 ml measured with 10% (w/w) Dextran (T500) solution. Carrier phase: KNO_3 (0.001 *M*)–FL-70 (0.01%, v/w)–bidistilled water. Flow-rate: 1 ml/min. Detector attenuation 100, stop flow time 40 min.

It must be noticed that the TiO_2 sample presents an almost resolved void-peak, when the stop flow time attains only 5 min, which is only 2% in value of the classically calculated relaxation time. Such a stop flow time reduction can be ascribed to the specific inlet geometry, for which sample particles reach the channel from the accumulation wall. With a longer stop flow time (20 min), a bimodal profile appeared. This can be due to particles of lower mass that need an increased relaxation time to reach their equilibrium position. This effect is confirmed by the curves relative to a 40-min relaxation time. However, when longer relaxation times are used bimodal fractogram profiles appeared less resolved (120 min). Consequently, an optimum relaxation time between 40 and 75 min was found. Such results suggest that the relaxation time can be considerably reduced if injections at low flow-rate is associated with the inlet at the accumulation wall. However, more systematic study in both GFFF and SdFFF are needed to formalise such a procedure. Otherwise, Fig. 3 shows the effectiveness of this injection methodology in the case of TiO_2, eluted by GFFF.

3.2.2. Sample loading capacity

At a constant injection loop volume, the sample injected mass depends on its concentration. Three

different sample concentrations were then eluted (0.25, 0.5 and 1%, w/w, suspended in the carrier phase). Relevant fractograms are shown in Fig. 4. A bimodal profile was observed only at 1% concentration. At lower sample concentration, fractions collection and further EM of fractions did not show significant shape dependent fractionation. However, particles in collected fractions were not sufficiently concentrated to allow for statistically significant measures of size and shape.

A concentration of sample of 1% can be therefore considered as the minimum concentration, able to give a characteristic bimodal GFFF profile, together with sufficient amounts of particles detected in the fractions.

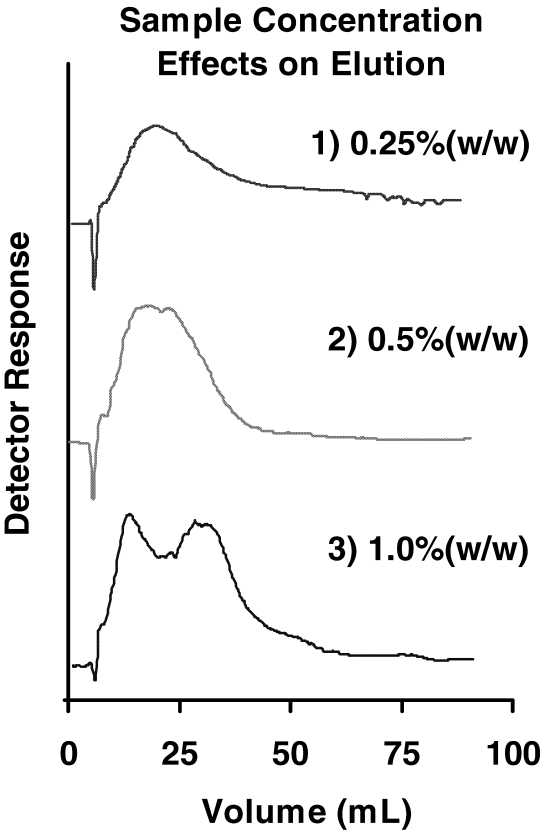

Fig. 4. Concentration effects on TiO_2 colloid elution profile in GFFF. Sample: 25 μl (0.25, 0.5, 0.01%, w/w) TiO_2 colloidal suspension in the carrier phase. Carrier phase: KNO_3 (0.001 *M*)–FL-70 (0.01%, v/w)–bidistilled water. Flow-rate: 1 ml/min. Detector attenuation 100.

3.2.3. Carrier phase electrolyte concentration

The effects of the electrolyte concentration in the carrier phase on the FFF elution of TiO_2 colloidal samples have been already described by Koliadima and Karaiskakis [16] using samples from different origins. They were equipped with SdFFF systems made of stainless steel channel walls [12]. They observed low recovery and a decreased retention at high KNO_3 concentration. These findings where described in terms of surface potential and Hamaker constant values for the onset of particle–particle and particle–wall interactions.

The experiments here performed in GFFF with polystyrene walls shows analogous features, as shown in the fractograms of Fig. 5.

At a high KNO_3 concentration (10^{-2} *M*), no TiO_2 elution signal was observed. Particle counting on fractions collected over the whole elution time showed low recovery values for the injected sample: 5±2% (n=5, σ). At lower ionic strength, elution was observed with an increased recovery, for $5\cdot10^{-3}$ *M* KNO_3 a recovery of 20±4% (n=5, σ), and for $2\cdot10^{-3}$ *M* an increased recovery of 40±6% (n=5, σ). With the ionic strength down to 10^{-3} *M* a bimodal profile appeared, with a 87±6% (n=5, σ) recovery. These findings are in accordance with what described by Koliadima and Karaiskakis [16] even though channel walls were of different nature. However, at the lowest ionic strength value of 10^{-4} *M* KNO_3 solution, a lower resolution of the bimodal profile was observed, lowering the possible separation of particle size and shape. Therefore an optimal ionic strength of 10^{-3} *M* was chosen to favour the separation in our equipment. In that case, it must be noticed that such a carrier phase used in a polystyrene channel will lead to a recovery ratio higher than that obtained from a stainless steel channel [16].

3.2.4. Carrier phase surfactant concentration

Surfactant concentration also plays a crucial role in giving its own contribution to total ionic strength as already described by Koliadima and Karaiskakis [16]. An additional role played by the surfactant is due to its adsorbsion on channel walls, as well as on particles. The most effective surfactant for TiO_2

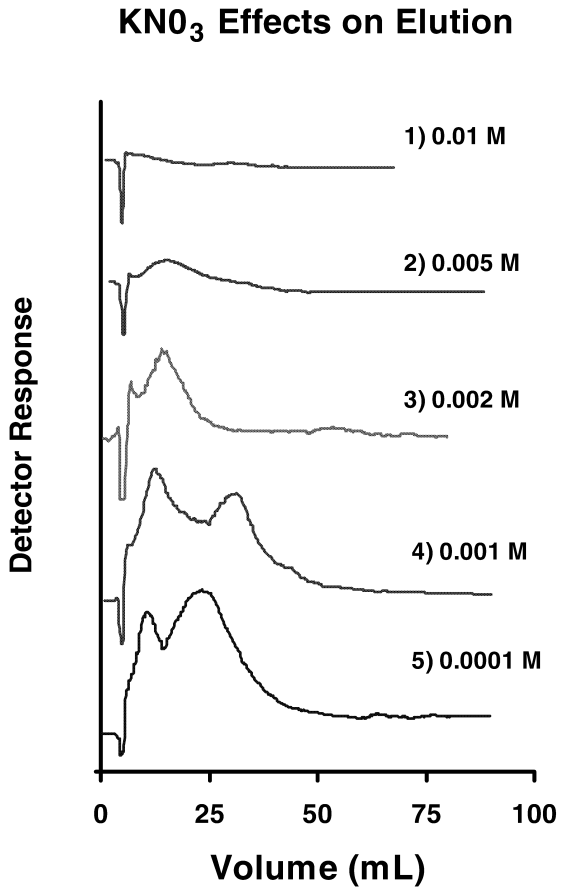

Fig. 5. Electrolyte effets on TiO_2 retention. Sample: 25 μl (0.25, 0.5, 0.1%, w/w) TiO_2 colloidal suspension in the carrier phase. Carrier phase: KNO_3 concentration varying from 0.01 *M* to 0.0001 *M*. –FL-70 (0.01%, v/v)–bidistilled water. Flow-rate: 1 ml/min. Detector attenuation 100, stop flow time: 40 min.

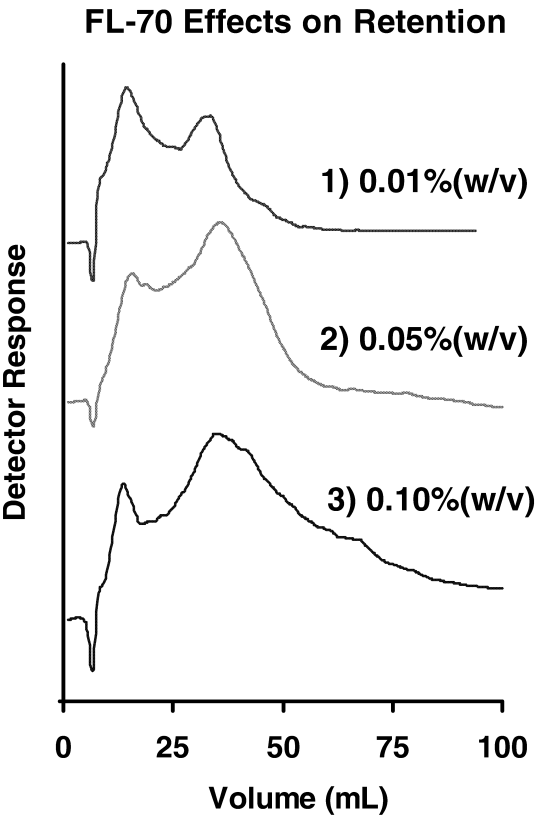

Fig. 6. Surfactant effets on TiO_2 retention. Sample: 25 μl (0, 0.5, 0.01%, w/w) TiO_2 colloidal suspension in the carrier phase. Carrier phase: KNO_3 (10^{-3} *M*)–FL-70 (%, v/w)–bidistilled water varying from 0.01 to 0.1%. Flow-rate: 1 ml/min. Detector attenuation 100, stop flow time: 40 min.

appeared to be FL70, a complex mixture of ionic and non-ionic surfactants. The characteristic effects of surfactant on SdFFF elutions of colloids have been extensively described by Mori et al. [17]. Surfactant concentration effects at a constant KNO_3 contribution to total ionic strength was then studied. The pH of the carrier phase ranged from 9.3 (FL-70, 0.01%, v/v, 10^{-3} *M* KNO_3) to 10.4 (FL-70, 0.1%, v/v, 10^{-3} *M* KNO_3) and the intermediate value was 9.6 (FL-70, 0.05%, v/v, 10^{-3} *M* KNO_3).

The obtained fractograms are shown in Fig. 6. A bimodal profile is systematically observed whatever the surfactant concentration. Moreover, retention ratio values of both populations appeared constant over a tenfold concentration range. However, the signal intensity as well as peak areas of sub populations appeared different. In order to check the origin of the difference between these fractogram profiles, we performed the collection of systematic fractions as the counting of particles. Results are summarised in Table 1.

Nevertheless, from data in Table 1, the signal difference cannot be only attributed to the effect of the surfactant on the selectivity of the trapping of different particles. This suggests a complex dependence of the RI response functions whose interpretation is beyond the scope of this paper [24].

Table 1
Fraction recovery at different surfactant concentration

Surfactant concentration	Fraction 1·100/total (%)	Fraction 2·100/total (%)
0.01%, pH 9.3	76±3 (n=3, σ)	24
0.05%, pH 9.6	75±4 (n=3, σ)	25
0.1%, pH 10.4	74±3 (n=3, σ)	26

Elution conditions described in Fig. 6. Optical microscopy analyses by means of an hematocytometer [5]. Surfactant effects on particle recovery. Total=(fraction 1+fraction 2) counts.

4. Conclusion

When compared to the sedimentation field flow fraction technique, that uses a multi-gravitational external field (SdFFF) [5], GFFF showed for TiO_2 particles, unique separation characteristics. This allowed to isolate two different populations of homogenous shape and size. Low flow-rate injection procedure with the inlet connected to the accumulation wall reduced drastically the required relaxation time.

When the different type of solvent and relevant size distribution analysed in this work are compared to the TiO_2 samples tested by Kirkland et al. [10] or Koliadima and Karaiskakis [16] in SdFFF, it is worthwhile to notice that a similar carrier phase composition were employed, even if channel walls of SdFFF were of different nature of those here used. Surfactant concentration and ionic strength for the mobile phase composition employed in these preceding reports can be, in fact, used qualitatively [10,16,17], for both GFFF and SdFFF techniques with polystyrene walls [5]. If the electrolyte concentration appeared here critical in terms of recovery and elution profile, the surfactant concentration could be associated to changes in fractogram profiles, that principally affected the bigger non-spherical particles.

The simplicity of the GFFF design is often limited by the impossibility to increase the external field intensity. It is also associated with a very low flow elution rate, leading to the general choice (when possible) of faster FFF techniques like flow FFF or SdFFF. Moreover, as for channel design, few information are available if we consider the optimisation of sample relaxation time process related to the inlet tubing position [25], which appears of critical importance for relaxation time reduction. However the separation performance of GFFF, already demonstrated by its wide range of applications, from mineral colloids as to living cell materials is too often underestimated. Otherwise, the limited availability of commercial FFF systems led scientists concerned with separation to build laboratory-made separators adapted to their own applications. In these regards, the versatility of GFFF, unique in terms of wall materials definition and channel design for a wealth of applications, is still under investigation.

References

[1] J.C. Giddings, G.C. Lin, M.N. Myers, J. Colloid Interf. Sci. 65 (1987) 67.
[2] J.C. Giddings, Science 260 (1993) 1456.
[3] K. Caldwell, G. Karaiskakis, J.C. Giddings, J. Virol. Methods 1 (1980) 241.
[4] S. Anger, K. Caldwell, H. Niehus, R.H. Müller, Pharm. Res. 16 (1999) 1743.
[5] Ph. Cardot, S. Rasouli, Ph. Blanchard, J. Chromatogr. A 905 (2001) 163.
[6] C. Contado, P. Reschiglian, S. Faccini, A. Zattoni, F. Dondi, J. Chromatogr. A 871 (2000) 449.
[7] E. Urbancova, A. Vacek, N. Novakova, F. Matulik, J. Chmelik, J. Chromatogr. 583 (1992) 27.
[8] A. Bernard, C. Bories, P. Loiseau, Ph. Cardot, J. Chromatogr. B 664 (1995) 444.
[9] M. Schure, M. Schimpf, P. Schettler, in: M. Schimpf, K. Caldwell, J.C. Giddings (Eds.), Field Flow Fractionation HandBook, Wiley-Interscience, New York, 2000, p. 31.
[10] J.J. Kirkland, S.W. Rementer, W.W. Yau, Anal. Chem. 53 (1981) 2038.
[11] L.E. McNeil, R.H. French, Acta Mater. 48 (2000) 4571.
[12] T. Moritz, G. Werner, G. Tomandl, M. Mangler, H. Eichler, U. Lembke, W. Hauffe, Wa. Kaysser, Mater. Sci. Forum 308–311 (1999) 884.
[13] N. Spanos, I. Georgiadou, A. Lycourghiotis, J. Colloid Interf. Sci. 156 (1993) 374.

[14] G. Bach, P. Abélard, P. Blanchart, J. Colloid Interf. Sci. 228 (2000) 423.
[15] T. Hoschino, M. Suzuki, K. Ysuwara, M. Takeuchi, J. Chromatogr. 400 (1987) 361.
[16] A. Koliadima, G. Karaiskakis, J. Chromatogr. 517 (1990) 345.
[17] Y. Mori, K. Kimura, M. Tanigaki, Anal. Chem. 62 (1990) 2668.
[18] A. Bernard, B. Paulet, V. Colin, Ph. Cardot, Trends Anal. Chem. 14 (1995) 266.
[19] T. Chianéa, S. Battu, Ph. Cardot, Talanta 51 (2000) 835.
[20] S. Rasouli, E. Assidjo, Ph. Cardot, J. Chromatogr. B (2001) in press.
[21] E. Assidjo, T. Chianea, M.F. Dreyfuss, Ph. Cardot, J. Chromatogr. B 709 (1998) 197.
[22] M. Hovingh, G. Thompson, J.C. Giddings, Anal. Chem. 42 (1970) 195.
[23] J. Janca, J. Chmelik, D. Pribylova, J. Liq. Chromatogr. 8 (1985) 2343.
[24] H. Coll, G.R. Fague, J. Colloid Interf. Sci. 76 (1980) 116.
[25] Ph. Cardot, T. Chianea, S. Battu, Encyclopedia of Chromatography, Marcel Dekker, New York, 2001.